

Brittle fracture of intact rocks: Theory

Assigned Reading:

Chapter 6, [Paterson and Wong, 2005], [Lockner, 1995]

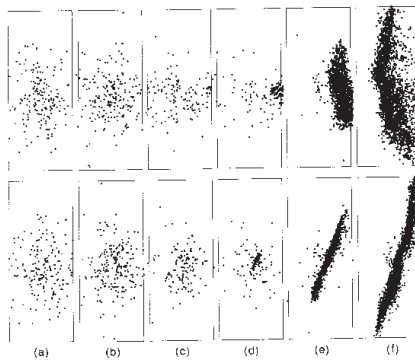
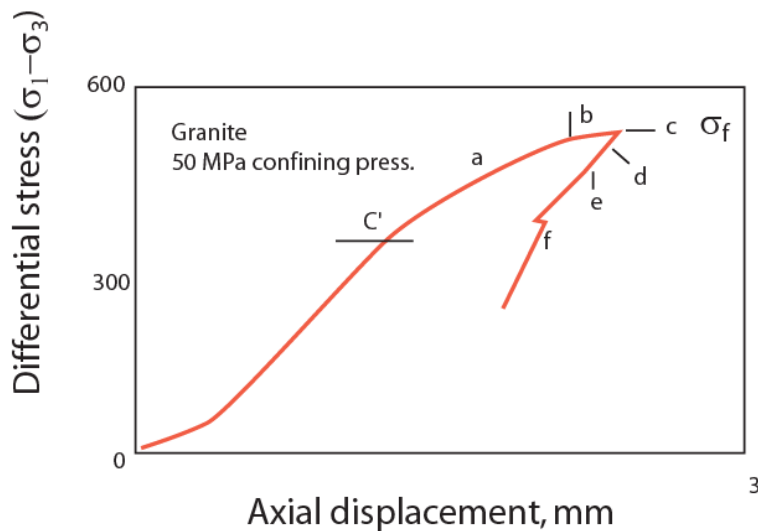
Resource reading:

[Hori and Nemat-Nasser, 1986; Kemeny and Cook, 1987a; Nematnasser, 1985; Rudnicki and Rice, 1975]

Typical Loading Curve:

Conventional Triaxial Compression of Intact Rock

Loading in cylindrical symmetry, i.e. conventional triaxial
Granite (Westerly) at 50 MPa conf. pressure
Initial loading is elastic with non-linear portion
After point C' strain becomes inelastic, "yield stress", σ_y .
Peak stress reached at "t c", "failure stress" σ_f

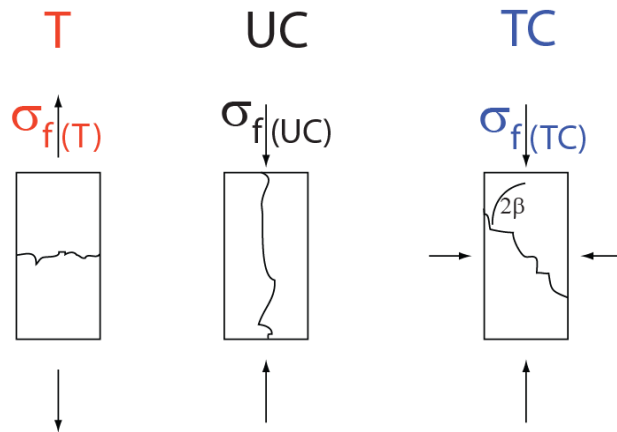
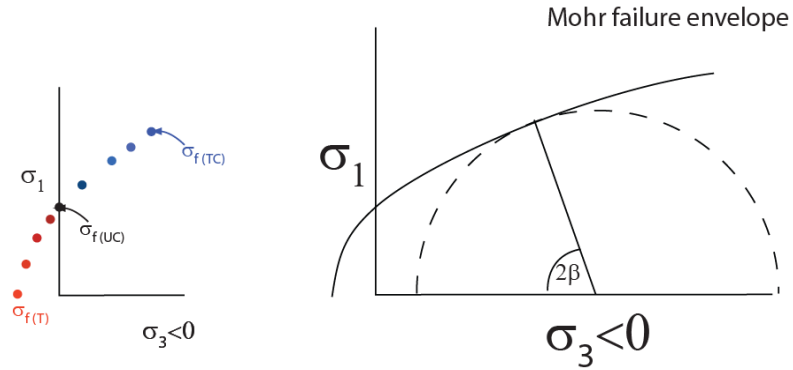


Acoustic emission pattern in sample during conventional triaxial loading at 50 MPa confining pressure. After Lockner, 1995. Each pattern occurred at a point in the loading curve indicated by letters a-f..

Mohr Failure Envelope:

Mohr-Navier-Coulomb Envelope:

Empirically, the failure stresses can be plotted as a function of the confining pressure



To first order, the failure stress is a linear function of pressure. The failure stress can be related approximately to the conf. pressure as

$$\sigma_{diff} = \sigma_{cohesive} + M\sigma_3$$

Mohr-Coulomb

where $\sigma_{diff} = \sigma_1 - \sigma_3$

Alternately, the shear stress on the failure plane at the instant of peak stress can be expressed at

$$\tau_{fracture\ plane} = \mu_i' \sigma_n_{fracture\ plane} + C$$

Mohr Failure Criterion

here the μ_i ' is called the internal coefficient of friction, by analogy to the coefficient of sliding friction. The prime symbol is included to indicate that the slope of the failure criterion is measured locally (small $\delta\sigma_3$).

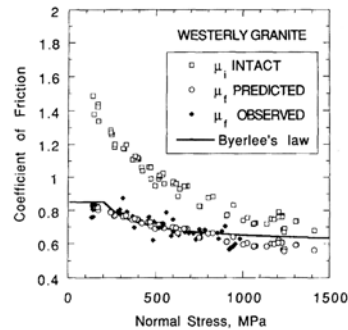
Needless to say the two quantities are related to each other,

$$\sigma_1 = \sigma_c + \left[(\mu_i^2 + 1)^{1/2} + \mu_i \right]^2 \sigma_3 \quad \text{Mohr Navier Coulomb FC}$$

In some cases, the failure criterion is given as a more (Mohr) complicated function of the mean stress

$$\sigma_1 - \sigma_3 = a(\sigma_1 + \sigma_3)^b$$

$$\sigma_1 - \sigma_3 = \left[a\sigma_c\sigma_3 + b\sigma_c^2 \right]^{1/2} \text{ and others (see Lockner, 1995).}$$



LOCKNER 133

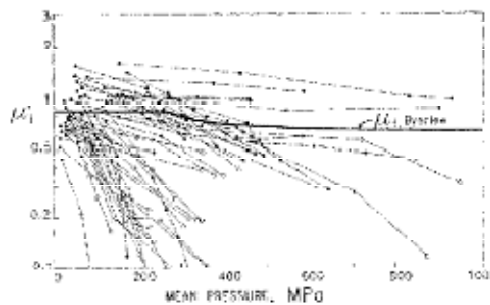


Fig. 5. Internal friction coefficient vs. mean pressure (for 1200) for compressive strength of rock types. Note: coefficient of friction is a function of the mean stress and the failure criterion. The general trend is as with the previous figure, but the horizontal line is a reference value for the internal friction coefficient, generally has low pressure sensitivity. These values appear on the lower part of the plot.

Theory:

At least two separate aspects of the failure curves need to be explained.

The yield point

The failure stress

Yield point:

Most silicates at low temperatures, laboratory loading rates, and confining pressures less than 500 MPa, fail by dominantly cataclastic processes, i.e., cracks form at local sites where stress heterogeneities or strain discontinuities are expected to develop.

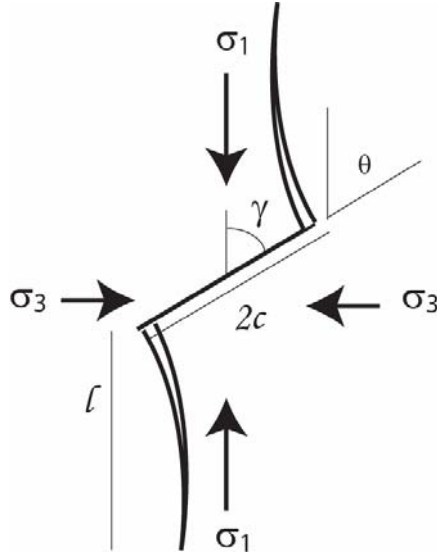
(see Tapponier and Brace, 1976 and Wong, 1982).

Such points of nucleation are often correlated with inclined flaws that might be expected to slip under shear loading.

After the yield point, dilatant cracking occurs, usually in an orientation such that cracks grow in length, more or less parallel to the greatest compressive stress (or in other words, with the normal to the crack plane parallel to the least compressive stress.) This orientation provides the least resistance to opening.

Stress Intensity:

Define some normalized parameters:



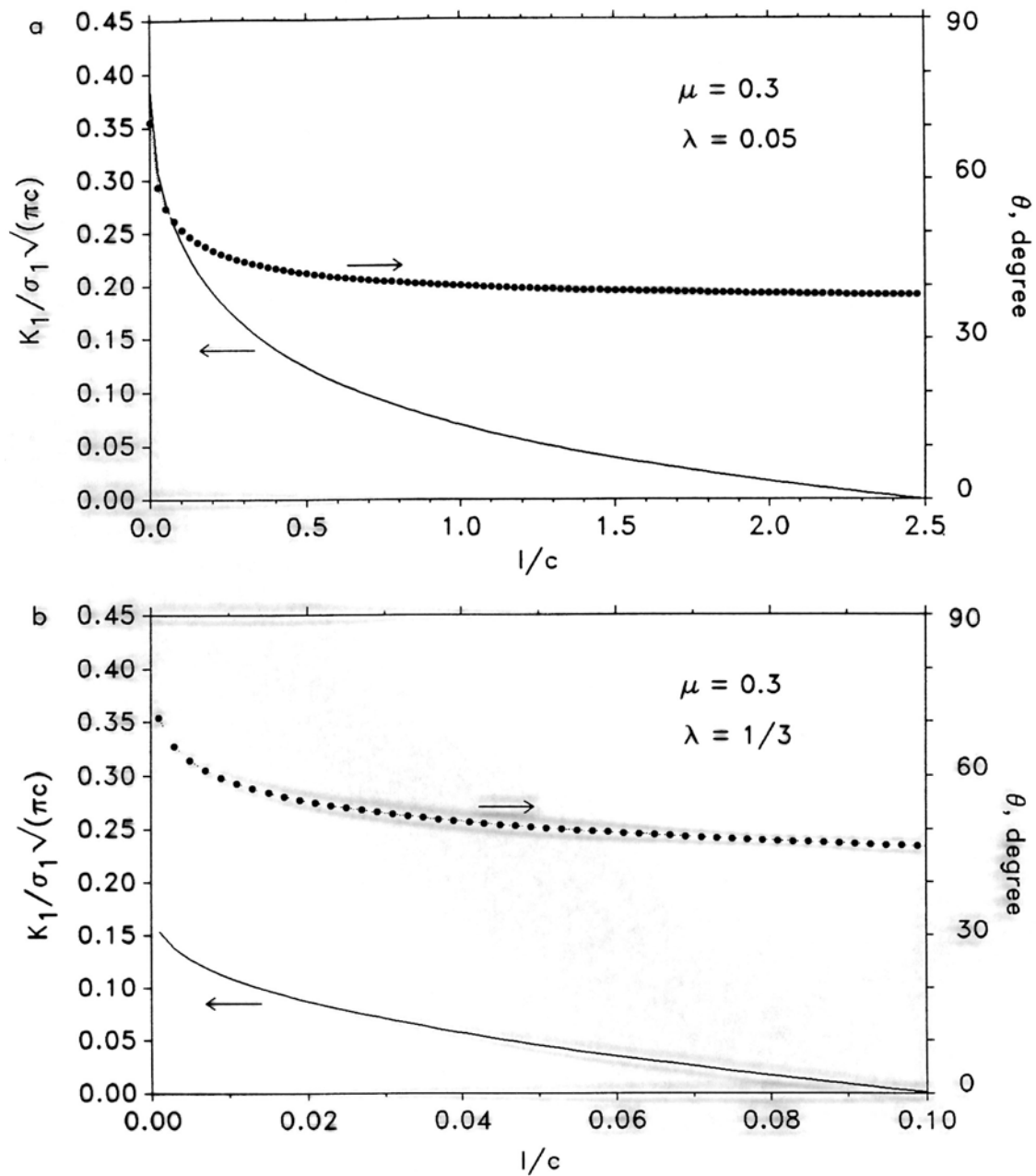
$\lambda = \frac{\sigma_{III}}{\sigma_I}$, a triaxiality parameter. Small for loading dominated by one axis, larger for confined stresses.

$L = \frac{l}{c}$, i.e., length of wing crack relative to initial sliding crack length.

$$L^* = \frac{8}{3\pi^2}$$

$$K_I = \sigma_I \sqrt{\pi c} \left\{ \left[(1-\lambda) \sqrt{1+\mu^2} - (1+\lambda)\mu \right] \cdot [\sin \theta] \cdot \left[\frac{1}{\pi \sqrt{L+L^*}} \right] - [1-\lambda] \cdot (1 - \cos 2(\theta - \gamma)) \frac{\sqrt{L}}{2} \right\}$$

1. Wing crack initiation starts at $\theta=70.5^\circ$, as L becomes large, orients itself to the greatest compressive stress.
2. Two terms in equation: wedging term, and tensile crack term.



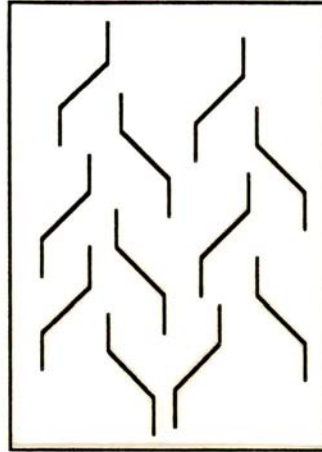
1. Increase in pressure decreases stress intensity.
2. Stress intensity decreases as (wing) crack lengthens.
3. Stabilizing process
4. Point of initial "yielding" depends on coefficient of sliding friction and pressure

Wing cracks with interactions:
i.e., Failure:

Two kinds of models: damage mechanics, stochastic computations.

Wing crack interaction (sample damage model)

Wing Crack Propagation (with interaction)



$$K_1 = \sigma_1 \sqrt{\pi c} \sqrt{\frac{2\varepsilon_0 (L + \alpha)}{\pi}} \sqrt{[1 - 8\varepsilon_0 \lambda (L + \alpha)^3][1 - 2\varepsilon_0 \lambda (L + \alpha)^3]}$$

Consider a staggered array of collinear cracks.
 Ensemble of optimally oriented sliding cracks, where

$$\varepsilon_o = c^2 N_A \quad \text{where } N_A = \# \text{ slide cracks / Area}$$

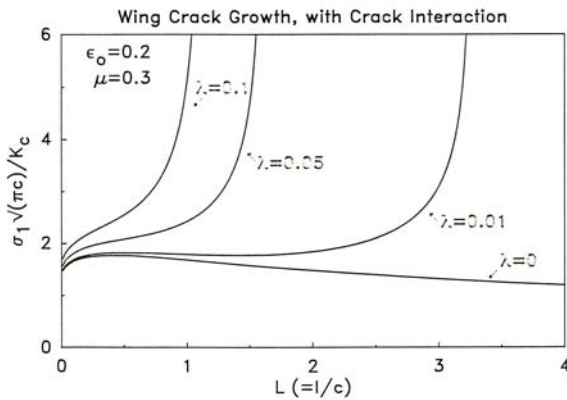
$$\alpha = \frac{1}{\sqrt{2}}$$

Then the appropriate damage parameter is

$$D = \pi (L + \cos \gamma)^2 \varepsilon_o$$

Notice that the spacing between the cracks

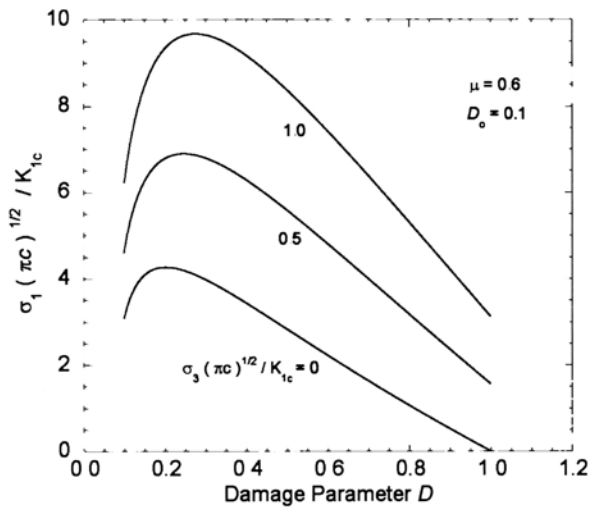
$$1/\sqrt{N_A}$$



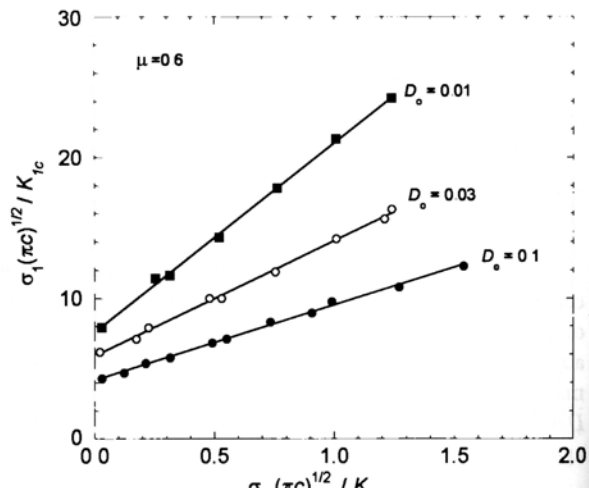
[Ashby and Sammis, 1990; Sammis and Ashby, 1986]

Stress intensity can increase with damage parameter

If loading stress are nomarlized by the critical stress intensity and plotted against damage parameter then,



If peak stress is identified as the failure strength:



And the failure strength can be given approximately as

$$\sigma_I = A(\mu, \epsilon_o) \sigma_{III} + B(\mu, \epsilon_o) \frac{K_{Ic}}{\sqrt{\pi C}}$$

Conclusions:

1. Qualitative explanation of dilatancy and failure.
2. Rational explanation of local stress state during dilatancy and failure.
3. Damage parameters explicitly identified.
4. Both c' and σ_f are related to fracture mechanics parameters including coeff. are related to fracture mechanics parameters including coeff of friction, K_{1c} , crack half length and so on.

Shortcomings:

1. Doesn't predict Mohr-Coulomb curvature.
2. Not tremendously sensitive to value of K_{1c}
3. Values of c interpreted from theory don't closely match the observed (inferred) values.
4. Dilatancy models that do not consider interaction require unusually low values of friction.
5. Doesn't include stochastic nature of actual damage (variations in length, random distributions, etc.).

Bibliography

- Ashby, M. F., and C. G. Sammis (1990), The damage mechanisms of brittle solids in compression, *Pure Applied Geophysics*, 133, 489-521.
- Horii, H., and S. Nemat-Nasser (1986), Brittle failure in compression: Splitting, faulting and brittle-ductile transition, *Phil. Trans. Royal Soc. London*, 319, 337-374.
- Kemeny, J. M., and N. G. W. Cook (1987a), Crack models for the failure of rocks in compression, *Proc. International Conference on Constitutive Laws for Engineering Materials*, 2, 879-887.
- Lockner, D. A. (1995), Rock failure, in *Rock Physics and Phase Relations: A Handbook of Physical Constants*, edited by T. A. Ahrens, pp. 127-146, American Geophysical Union, Washington, DC.
- Nematnasser, S. (1985), Mechanics of Brittle Failure in Compression, *Computers & Structures*, 20, 235-237.
- Paterson, M. S., and T.-f. Wong (2005), *Experimental rock deformation - The brittle field*, Second ed., 347 pp., Springer Verlag, Berlin, New York.
- Rudnicki, J. W., and J. R. Rice (1975), Conditions for the localization of deformation in pressure sensitive dilatant materials, *Journal of the Mechanics and Physics of Solids*, 23, 271-394.
- Sammis, C. G., and M. F. Ashby (1986), The failure of brittle porous solids under compressive stress states, *Acta Metallurgica*, 34, 511-526.